Inorganic Chemistry

Article

pubs.acs.org/IC

Aqueous Hafnium Sulfate Chemistry: Structures of Crystalline Precipitates

Ali Kalaji and L. Soderholm*

Chemical Sciences and Engineering Division, Argonne National Laboratory, 9700 S Cass Avenue, Argonne, Illinois 60439, United States

Supporting Information

ABSTRACT: Crystalline precipitates resulting from the hydrolysis and subsequent condensation of Hf^{IV} aqueous acidic solutions at 60−95 °C are examined and compared. By varying the concentrations of the acid and sulfate source, a variety of complex hafnium-oxo-hydroxo-sulfate clusters are isolated and structures accessed. Four novel compounds were discovered, while the structures of two known compounds, an 18-mer and a planar hexamer, were updated. In total, the compounds described herein each contain one of four cluster architectures: 18-mer, 11-mer, nonamer, and planar hexamer. In addition, one compound contains small amounts of 19-mers together with 18-mers. As well as examining the individual structure of each complex cluster, we relate them to one another, as well as to the dense phases of HfO_2, to gain an understanding of their formation and stability. Finally, the solution conditions under which each cluster forms are identified by plotting the crystallization regions of each cluster against acidity and sulfate concentration. Most clusters form under slightly acidic conditions, in decreasing size as the sulfate concentration is raised. The flat hexamer is the single exception; it appears to require more acidic solutions. The degree of hydroxo- versus oxo-bridges with changing solution conditions is assessed within the broader context of the condensates. Of specific interest is the identification of these products as they relate to the use of hydrolysis reactions in designing new materials.

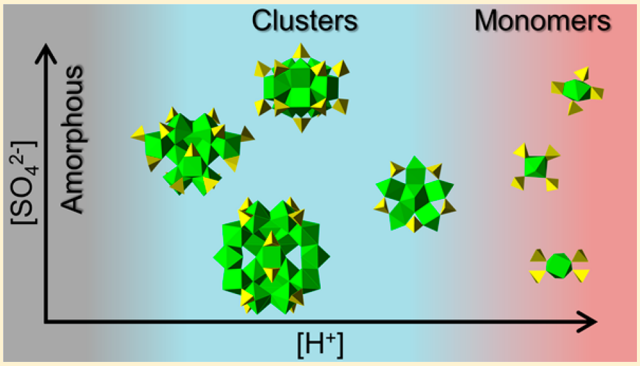

INTRODUCTION

Higher-valent cations, including V^{V}, Mo^{VI}, and W^{VI}, undergo hydrolysis and subsequent condensation reactions in aqueous solution that can be controlled to yield monodisperse, oxo-bridged, polyoxometalate clusters with a broad array of targeted applications.[1,2] In contrast, lower-valent ions are softer, and their condensation often results in chemically and structurally ill-defined dihydroxo- or oxo/hydroxo-bridged precipitates. Work with hydrolyzed tetravalent ions (M^{IV}), including Zr^{IV},[3−6] Hf^{IV},[7] and Th^{IV}−Pu^{IV},[8,9] is revealing that under select aqueous conditions it is possible to precipitate crystalline oxo/hydroxo clusters, at least some of which preform in solution. With the goal of directly harnessing hydrolysis chemistry as an alternate route to materials syntheses, we are interested in probing the attributes of M^{IV}-ions and how they combine with underlying solution conditions, including pH, concentration, temperature, and the choice of counterion, to influence the precipitates that form.

Recent work on the crystallization of Th^{IV}−Pu^{IV} clusters[10−15] indicates that small changes in metal-ion hardness (charge-to-radius ratio) or electronegativity can favor oxo-bridged species over their hydroxo-bridged counterparts, indicating a tendency toward oxolation over olation condensation. The softest tetravalent ion on the periodic table, Th^{IV}, forms hydroxo-bridged dimers or larger oxyhydroxo-bridged oligomers,[10] the largest reported is a selenate-stabilized octamer.[13] In contrast, Pu^{IV}, which is about 9% harder, exhibits predominantly oxo-bridged nanoparticles, the largest of which is the 38-mer $[Pu_{38}O_{56}]^{40+}$,[11,16] seen in solution and crystallized as hydrated Li salts of chloride stabilized clusters. Work with Zr^{IV} and Hf^{IV} are not consistent with the trends seen for the 5f series. Zr^{IV} and Hf^{IV}, both harder than Pu^{IV}, have a preponderance for hydroxo-bridged oligomers in solution.[3,6,7] Furthermore, there is evidence that bidentate anions, such as sulfate, selenate, or carboxolate, influence precipitate structure, a phenomenon also seen for Th^{IV}.[17]

To further the understanding of the role played by hardness on the condensation products that precipitate, we extend our studies from Th^{IV}, the softest of the tetravalent ions stable in aqueous solution, to Hf^{IV}, which is one of the hardest such ions. We recently investigated a series of Hf^{IV} solutions with varying sulfate concentration to provide a molecular understanding of Hf aqueous speciation and how it changes with anion concentration.[7] Crystals were isolated from the end-member solutions and their correlations compared with those found in solution using high-energy X-ray scattering (HEXS). For example sulfate-free aqueous solution Hf^{IV} is known to form

Received: July 29, 2014
Published: October 9, 2014

   dx.doi.org/10.1021/ic501841e | Inorg. Chem. 2014, 53, 11252−11260

Table 1. Summary of the Hf Clusters in Compounds 1−7[a]

compd	cluster	formula	notes	ref
1	18-mer	$[Hf_{18}O_{10}(OH)_{26}(SO_4)_{12.7}(H_2O)_{20}]Cl_{0.6}\cdot nH_2O$	previously reported: Cl^- located in voids	22
2	18-/19-mer	$[Hf_{18}O_{10}(OH)_{26}(SO_4)_{13}(H_2O)_{22}]_{0.88}$ $[Hf_{19}O_{11}(OH)_{27}(SO_4)_{13}(H_2O)_{22}]_{0.12}$ $(NH_4)_{5.64}(SO_4)_{2.88}\cdot nH_2O$	related to 1 but larger unit cell; no intercluster sulfate connectivity	
3	11-mer	$[Hf_{11}O_7(OH)_{11}(SO_4)_{15}(H_2O)_6](NH_4)_{11}\cdot nH_2O$		
4	11-mer	$[Hf_{11}O_7(OH)_{11}(SO_4)_{15}(H_2O)_6](NH_4)_{13}SO_4\cdot nH_2O$		
5	nonamer	$[Hf_9O_8(OH)_6(SO_4)_{14}](NH_4)_{14}\cdot nH_2O$	reported recently	24
6	planar hexamer	$[Hf_6O_5(SO_4)_{10.5}(H_2O)_{6.5}](NH_4)_7\cdot nH_2O$	previously reported: structure and stoichiometry modified	21
7	planar hexamer	$[Hf_6O_5(SO_4)_{10.5}(H_2O)_{6.5}](NH_4)_7\cdot nH_2O$		

[a]Compositions of discrete-cluster units are given in square brackets. References are included for previously published structures.

the square tetrameric cation $[Hf_4(OH)_8(H_2O)_{16}]^{8+}$,[3,7,18] a species known to form even under highly acidic conditions. Although there is evidence that it is in equilibrium with larger clusters in solution, only the tetrameric hydroxo-bridged cluster was isolated in the solid state. Under the influence of the strongly coordinating sulfate ligand a diverse aqueous chemistry unfolds, somewhat similar to that seen for Zr^{IV}, in which competing species are identified.[6,19−22] This chemistry is reflected in the solid state, where hafnium forms a variety of uncommon cluster architectures, including the 18-mer[22] and a planar hexamer[21] with one central Hf surrounded by five other Hf atoms arranged in a pentagon. More recently, a 17-mer composed of the 18-mer with one missing Hf was also identified.[23] A nonamer has also been reported with a rare, cage-like core structure that has only been observed in the aqueous chemistry of Bi^{3+}.[24] The diversity seen in crystalline precipitate structures supports the previous conclusion that there are complex equilibria in Hf-sulfate solutions that can be manipulated to favor specific species.[7]

Herein we extend the study of Hf^{IV} hydrolysis chemistry to probe the influence of aqueous solution pH together with sulfate concentration on the oligomeric species that precipitate. To aid in unraveling the complex chemistry and informing future analyses of solution data, we have structurally characterized crystalline precipitates. The result of this study is the identification of several new Hf-sulfate compounds. Their structures are discussed in the context of the solution conditions from which they were isolated. It is our expectation that these results will inform efforts directed toward untangling the complex hydrolysis chemistry and resultant ion correlations seen in solution. This is a necessary step toward rational approach Hf-oxide syntheses such as those encountered in recent endeavors to replace SiO_2 gate dielectrics in field-effect transistors by other high-k materials, including HfO_2.[25,26]

EXPERIMENTAL METHODS

Crystal Growth. All compounds reported herein were crystallized from aqueous solutions. $HfOCl_2\cdot 8H_2O$ (Alfa Aesar, ≥98%), H_2SO_4 (Fisher Scientific, Optima), HCl (Fisher Scientific, Optima), and $(NH_4)_2SO_4$ (Sigma-Aldrich, 99.999%) were used as purchased. A series of solutions were prepared whereby the acid concentrations and $(NH_4)_2SO_4$ were varied systematically in order to map the crystallization regions of the different compounds. The concentration of the hafnium salt was fixed at 0.3 molal throughout. All concentrations were determined in molal (m or mol kg^{-1}) for simplicity and reproducibility. Each solution contained 1 g of water (deionized, 18.2 MΩ·cm) and was placed in a closed 5 mL glass vial. Solutions were heated at 60−95 °C by placing the reaction vials in a forced convection oven. Control reactions were also prepared where the solutions were left to stand in closed vials at room temperature. Far better results were achieved from the reactions carried out at elevated temperatures compared with room temperature syntheses. Heating was required for the crystallization of some compounds (as detailed below), while other compounds formed at room temperature but resulted in crystals that were less suitable for SCXRD due to their small crystal size and lower quality (irregular shapes and diffraction-peak widths). Nevertheless the unit cells were the same for all crystals measured, irrespective of their synthesis temperature. In order to allow for slow crystal growth, solutions were heated at the lowest temperature at which crystallization occurs. Initially, all solutions were kept at 60 °C for 1 week. Following this heating step, any solutions lacking crystals were heated at 80 °C for 1 week. Once again, if no crystallization occurred, the temperature was raised to 95 °C for 2 weeks. After this point, any solutions without crystals were deemed to be outside the crystallization regions (below 100 °C) for the purpose of this study. The synthesis of the compounds reported herein is highly reproducible; see the Supporting Information for specific synthetic details of each compound. $(NH_4)_2SO_4$ was used as the sulfate source due to its high solubility in water relative to M_2SO_4 (M = Li, Na, K, Rb). The use of Cs_2SO_4 (also highly soluble) resulted in much faster crystal formation (less than 24 h). These crystals were always of low quality making their molecular structure difficult to resolve. The two $(NH_4)_2SO_4$ studies were conducted, as explained below.

Study 1: Sulfuric Acid. This study was conducted using H_2SO_4 to adjust the acidity and $(NH_4)_2SO_4$ to control the sulfate concentration. $[SO_4]^{2-}$, $[H_3O]^+$, and $[NH_4]^+$ concentrations were varied while Hf^{IV} and Cl^- concentrations remain fixed (0.3 and 0.6 m, respectively). Clear crystallization regions were identified using this method despite the fact that adjusting the H_2SO_4 concentration changes both acidity and the $[SO_4]^{2-}$ concentration. Multiple crystals from each solution were examined using single-crystal X-ray diffraction and Raman spectroscopy to confirm phase purity and homogeneity. There was clear evidence of co-crystallization from a few solutions as described below, but for the majority of solutions the crystals were phase pure.

Study 2: Hydrochloric Acid. In this case, HCl was used to adjust the acidity while $(NH_4)_2SO_4$ controlled the sulfate concentration. Here, variations in the concentrations of $[SO_4]^{2-}$, $[H_3O]^+$, $[NH_4]^+$, and Cl^- occurred while the Hf^{IV} concentration was fixed at 0.3 m. This approach enabled the adjustment of acidity without affecting the $[SO_4]^{2-}$ concentration. However, at high acid concentration, the effect of Cl^- on the crystallization regions was anticipated to become more pronounced. Once again, the crystallization regions were clearly identified. The crystal structures of the compounds obtained herein were identical to those from study 1.

Note that, for simplicity, the crystallization regions are reported in terms of the starting concentrations of the acids and sulfate salts since the presence of partially deprotonated $[HSO_4]^-$ species were also expected.

Single Crystal X-ray Diffraction (SCXRD) and Structure Determination. Reflections were collected on a Bruker AKX SMART diffractometer equipped with an APEXII CCD detector using Mo Kα radiation. The data were integrated and corrected for absorption using the APEX2 suite of crystallographic software.

dx.doi.org/10.1021/ic501841e | Inorg. Chem. 2014, 53, 11252−11260

Structures were solved by direct methods and refined using XShell (SHELXL-97).

Raman Spectroscopy. Raman spectra of compounds **1**–**4**, **6**, and **7** were collected using a Renishaw inVia Raman Microscope with an excitation wavelength of 532 nm at 50% laser power. Each spectrum consists of the summation of 10 acquisitions.

RESULTS

Solid-State Structures. Seven compounds were crystallized and identified, of which only three had been previously reported, as summarized in Table 1. In total, five cluster architectures were found in these compounds, all containing Hf oxo/hydroxo-clusters that have sulfate-bridged Hf atoms. In all clusters, the core is composed of Hf atoms bridged by O^{2-} or OH^- ligands, while sulfate ligands cap the surfaces of the clusters in various bridging (μ_2 or μ_3) and chelating (η_1 or η_2) modes. With the exception of the nonamer, all clusters also contain H_2O ligands bound to Hf. Where present, Cl^- and $[NH_4]^+$ ions act as counterions and are found in the voids between the clusters. All structures involve networks of hydrogen-bonding interactions between OH^-, H_2O, and $[SO_4]^{2-}$ groups in the clusters and H_2O, $[NH_4]^+$, and $[SO_4]^{2-}$ species in the voids. The crystal structures of the four main clusters are illustrated in Figure 1. The structure of

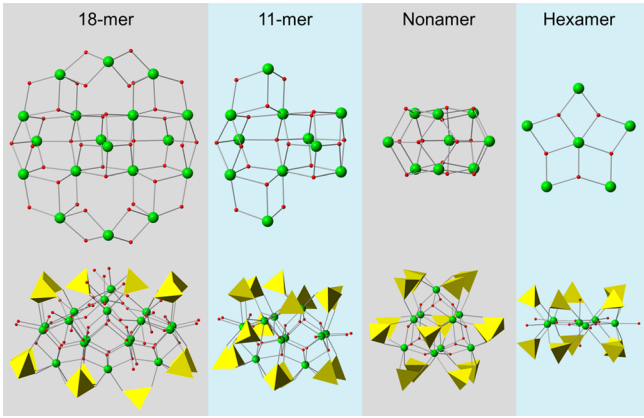

Figure 1. Illustration of the clusters found in the HfO_2–H_2SO_4–HCl–$(NH_4)_2SO_4$ system. The top row shows the cluster cores containing only Hf^{4+} with O^{2-} and OH^- ligands, whereas in the bottom row the coordinated sulfate and H_2O ligands are added. Hafnium and oxygen are shown in green and red, respectively, while $[SO_4]^{2-}$ ligands are represented by yellow tetrahedra. Protons and noncoordinating groups (Cl^-, $[NH_4]^+$, $[SO_4]^{2-}$, and H_2O) are omitted for clarity.

the fifth cluster (19-mer) is described separately below since it is derived from the 18-mer and is observed less frequently. Concise structural descriptions are provided for compounds **1**–**7** below. For detailed crystallographic information, see the Supporting Information.

Essential crystallographic data and refinement parameters are presented in Table 2. The structures of the cluster cores in **1**–**7** were elucidated using standard SCXRD techniques, exhibiting relatively small atomic displacement parameters and no disorder, with the only exception occurring for compound **2**, where a fraction of the clusters contain a 19th Hf atom. Within each core, differentiating between oxo and hydroxo groups was achieved using bond-valence sums.[27] There was no ambiguity between these assignments as all μ_2 ligands could only be OH^- groups; the few μ_3-OH^- ligands detected protrude significantly out of the Hf_3 plane relative to μ_3-O^{2-}, and all μ_4 ligands must be O^{2-} based on their Hf–O bond distances. The sulfate ligands, located on the outer edges of the clusters, exhibit some disorder that was modeled in the refinements but not depicted in Figure 1 for simplicity. This was particularly prevalent for the two planar hexamer compounds, **6** and **7**. The complexity of all these structures as well as the contrast between the heavy Hf atoms and light O atoms made locating all the disordered H_2O molecules in the voids between the clusters challenging. Weak electron density peaks were detected in the voids between the clusters, but structural disorder together with the presence of (ordered) counterions prohibited the effective assessment of corresponding disordered waters using available structural characterization tools such as SQUEEZE. Those H_2O molecules that were located in the voids are represented in the molecular formula included in the CIF data in the Supporting Information and in Table 2. However, the total number of H_2O molecules present in the voids remains uncertain, as indicated in Table 1. All compounds reported herein involve typical Hf–O bond distances in the 2.00–2.40 Å range. The Hf–Hf distances were also typical, ranging from 3.50–3.70 Å in hydroxo-bridged Hf–Hf, down to 3.34 Å in the planar hexamer.

The structure of the 18-mer cluster has been previously determined for both hafnium[22] and zirconium.[20] In those reports, the 18-mers were obtained from the HfO_2–H_2SO_4[22] and ZrO_2–H_2SO_4–HCl[20] systems. Being the only compound we found not containing $[NH_4]^+$, **1** is essentially isostructural to the previously reported Hf 18-mer. The only difference found was the presence of a Cl^- anion in the voids in **1** complemented by a lower occupancy for two sulfate groups (S2). In this compound, the clusters form a hexagonal arrangement with chains running along the *z*-axis linked by bridging μ_2-sulfates. The incorporation of a small amount of $(NH_4)_2SO_4$, however, leads to the formation of compound **2**. Despite crystallizing in the same unit cell and similar cluster packing as **1**, compound **2** displays some interesting differences. Approximately 12% of the clusters in **2** contain a 19th Hf atom (Hf12) attached to the core at one end by one μ_4-oxo, two μ_2-hydroxo, and two μ_2-sulfate ligands (see Figure 2). The sulfate group bridging the 18-mers in **1** along the *z*-axis (see Figure 2) is absent from **2**, replaced instead by two bound water ligands and three unbound sulfates in the same region between the clusters. In **1**, the distance between the two intercluster sulfate-bridged Hf atoms is 6.69 Å, whereas the removal of this bridge in **2** increases this distance to 7.77 Å. No Cl^- anion was located in the voids in **2**. The differences between **1** and **2** manifest themselves in a 14.5% expansion in the unit cell volume for the latter. The 18-mer clusters in **1** carry a slight cationic charge (+0.6), whereas those in **2** are neutral. The 19-mers are only slightly cationic (+0.12). The formation of the 19-mer, albeit rare, reflects the propensity of Hf^{IV} to polymerize in aqueous solutions. The 18-mer and 19-mer clusters are expected to be in equilibrium, with the site of addition of Hf12 promoted by the disorder in the two S2 sulfates.

Compounds **3** and **4** contain a new 11-mer cluster. The core of this cluster is composed of a fragment of the 18-mer cluster core, as demonstrated in Figure 1. This core contains six Hf atoms arranged in an octahedral hexamer surrounded on one side by a 5-Hf fragment of the 12-Hf ring found in the 18-mer. Oxo- (μ_4 and μ_3) and hydroxo- (μ_3 and μ_2) bridges connect all hafnium atoms in the core, while six H_2O ligands complete the coordination shell of four Hf atoms. Unlike the 18-mer cluster,

dx.doi.org/10.1021/ic501841e | Inorg. Chem. 2014, 53, 11252–11260

Table 2. Crystallographic Data for Compounds 1−4, 6, and 7

	1	2	3	4	6	7
formula	$Cl_{0.6}H_{126.53}Hf_{18}O_{137.07}S_{12.7}$	$H_{116.92}Hf_{18.12}N_{5.64}O_{134.26}S_{15.88}$	$H_{96}Hf_{11}N_{11}O_{98.50}S_{15}$	$H_{104}Hf_{11}N_{13}O_{102.50}S_{16}$	$H_{43}Hf_{6}N_{7}O_{54.50}S_{10.50}$	$H_{49}Hf_{6}N_{7}O_{57.50}S_{10.50}$
cryst size (mm^3)	0.039 × 0.049 × 0.177	0.034 × 0.060 × 0.149	0.108 × 0.065 × 0.045	0.113 × 0.130 × 0.272	0.040 × 0.045 × 0.120	0.037 × 0.077 × 0.084
T (K)	100(2)	100(2)	100(2)	100(2)	100(2)	100(2)
λ (Å)	0.710 73	0.710 73	0.710 73	0.710 73	0.710 73	0.710 73
cryst syst	hexagonal	hexagonal	triclinic	monoclinic	orthorhombic	orthorhombic
space group	$P6_3/m$	$P6_3/m$	$P\bar{1}$	$P2_1/n$	$Pnma$	$Pmmn$
a (Å)	33.7242(12)	34.763(2)	15.1165(8)	14.9489(5)	22.5768(6)	19.0716(7)
b (Å)	33.7242(12)	34.763(2)	24.5806(13)	30.1150(10)	9.8962(3)	9.9058(4)
c (Å)	17.3577(6)	18.7107(13)	25.0808(13)	23.2134(8)	23.7620(6)	14.1053(5)
α (deg)	90	90	88.4626(8)	90	90	90
β (deg)	90	90	81.5081(8)	102.3600(10)	90	90
γ (deg)	120	120	87.5482(8)	90	90	90
V ($Å^3$)	17 096.5(14)	19 582(3)	9206.7(8)	10 208.1(6)	5309.0(3)	2664.77(17)
Z	6	6	4	4	4	2
fw(g/mol)	5961.71	6088.29	4271.11	4403.31	2420.98	2475.03
calcd density (g cm^{-3})	3.474	3.098	3.081	2.865	3.029	3.085
abs coeff μ (mm^{-1})	16.717	14.758	12.828	11.597	12.230	12.190
total no. reflns	297 531	338 257	155 246	178 352	92 221	46 419
unique reflns	19 831	22 530	60 624	35 810	10 329	5289
R1 [$I > 2\sigma(I)$]	2.63%	4.39%	5.42%	4.68%	4.88%,	2.23%
wR2	6.43%	11.49%	12.11%	11.87%	10.25%	5.57%
largest diffraction peak and hole (e $Å^{-3}$)	7.450, −5.792	6.421, −3.467	9.264, −3.615	8.557, −5.421	5.616, −3.807	2.839, −2.212
GOF	1.041	1.119	1.130	1.090	1.261	1.113

dx.doi.org/10.1021/ic501841e | Inorg. Chem. 2014, 53, 11252−11260

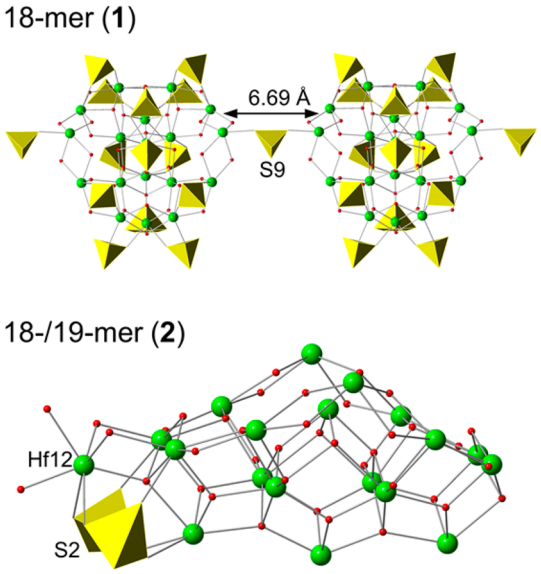

Figure 2. Differences between compounds **1** and **2**. (Top) Figure highlighting the μ_2-sulfate bridge present only in **1** that links the 18-mers along the *z*-axis. (Bottom) The additional 19th Hf atom is present only in 12% of the clusters in **2**.

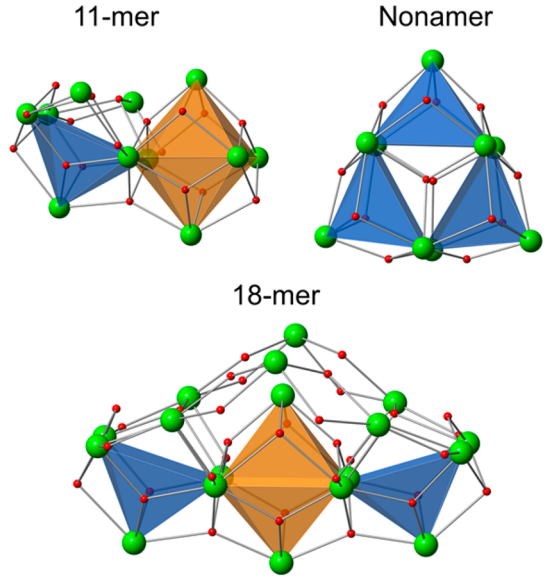

Figure 3. Illustration showing the square-based pyramids (blue) and hexamers (orange) present in three hafnium cluster cores.

where two Hf atoms are 7-coordinate and the remaining 16 are 8-coordinate, the 11-mer contains only 8-coordinate Hf. The higher intracluster sulfate-to-hafnium ratio for the 11-mers (1.36) versus the 18-mers (0.71−0.72) is a result of the more extensive sulfate complexation surrounding the 11-mer core. It appears that the added sulfate complexation impedes the growth of the larger 18-mer core resulting in the 11-mer fragment. Also, unlike the neutral/slightly cationic 18-mer cluster, the 11-mer cluster is strongly anionic, with a charge of −11. The 11-mer contains five bidentate (η_2) sulfates, eight μ_2-sulfates, and two μ_3-sulfates. The clusters in **3** and **4** are identical, and there is no intercluster connectivity. The only differences between these two compounds involve the cluster packing and void species. Both compounds contain four clusters per unit cell, and yet the unit cell volume in **3** is smaller than that of **4**. This results in slightly tighter packed clusters in **3**. There is one additional uncoordinated sulfate anion per cluster in the voids in **4**.

Given the formation of the 11-mer cluster, it could be expected that increasing the sulfate complexation further would result in an isolated octahedral hexamer cluster, since this can be regarded as an even smaller stable fragment of the 18-mer. However, such an increase resulted in the formation of a nonamer (**5**), with a structure seemingly unrelated to the 18-mer and a sulfate-to-hafnium ratio of 1.56. We recently reported this novel structure and its resemblance to two bismuth clusters.[24] The cage-like nonamer core comprises a tricapped trigonal prism of nine Hf atoms with D_{3h}-like symmetry. All oxo- and hydroxo-bridges in **5** are triply bridging (μ_3), and there are no H_2O ligands coordinated to Hf. Although the nonamer does not contain a hexameric unit, it does contain three edge-sharing square pyramids similar to those found in both 11-mers and 18-mers (see Figure 3). These pentamer motifs are structurally related to the octahedral hexamer, formed by the omission of a single axial Hf atom from the hexamer. Both motifs can thus be regarded as building blocks for the high temperature tetragonal and cubic HfO_2 phases, while the room temperature monoclinic phase contains distorted square-based pyramids and hexamers due to the lower 7-fold coordination around hafnium.

The planar hexamer found in compounds **6** and **7** is structurally unrelated to the octahedral-hexamer motif discussed herein and ubiquitous in tetravalent metal-ion hydrolysis chemistry.[4,9,14,15,28−30] All six Hf atoms and the five oxo ligands that connect them lie in the same plane, with one Hf atom at the center surrounded by five Hf atoms arranged in a nearly regular pentagon. Each of the five outer Hf atoms have one in-plane H_2O coordinated ligand pointing away from the center of the pentagon, while the central Hf has two axial H_2O ligands above and below the plane. 25% of the axial H_2O ligands are replaced by disordered monodentate (η_1) nonbridging sulfates coordinated to the central hafnium atom (not depicted in Figure 1). The remaining 10 sulfate ligands are doubly bridging, arranged in two halos above and below the Hf-oxo core plane. The hexamers in **6** and **7** are almost identical bar variations in the disorder of the sulfates. The unit cell volume in **7** is half that of **6**, with only two clusters per unit cell in the former. This is due to a more ordered packing of the clusters in **7** (see Supporting Information). Compound **6** was reported previously,[21] although our refinement revealed a few minor differences with the reported structure. We found that all five bridging oxygen atoms are oxo ligands based on bond-valence sums.[27] The previous report suggested the presence of one hydroxo bridging ligand based on charge-balance requirements. The partially occupied axial sulfate and two extra $[NH_4]^+$ ions in **6** were not identified in the previous report.

The planar hexamer does not contain any structural motif found in the other clusters. However, given the prevalence of the 7-fold coordination of Hf in this cluster, it is worth relating its structure to that of the monoclinic HfO_2 phase[31] (also exclusively 7-fold Hf). The five outer Hf atoms in the hexamer are found in slightly distorted monocapped trigonal prisms. The same applies to the $[HfO_7]$ polyhedron found in HfO_2, although the distortion is more pronounced in the latter.[31] The central Hf atom in the hexamer is surrounded by a nearly perfect pentagonal bipyramid of oxygen atoms. This unusual coordination is not found in the oxide structures of Hf, but instead was found for a sulfate compound.[32] Despite this, the

dx.doi.org/10.1021/ic501841e | *Inorg. Chem.* 2014, 53, 11252−11260

$[HfO_7]$ polyhedron in monoclinic-HfO_2 may also be viewed as a strongly distorted version of the pentagonal bipyramid, as demonstrated in Figure 4. From this viewpoint, the "central" Hf

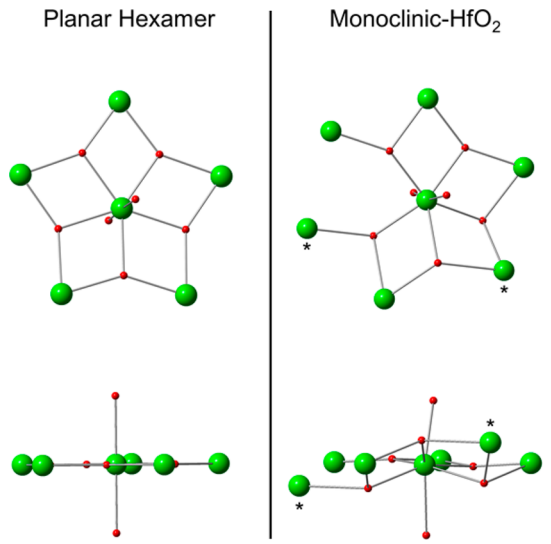

Figure 4. Comparison of the planar hexamer core with a fragment of the monoclinic phase of HfO_2. The two Hf atoms marked with asterisks lie substantially outside the main Hf "plane".

atom in HfO_2 is linked to six other Hf atoms by oxygen bridging ligands. Four of these Hf atoms form an almost perfect plane with the central Hf. The axial O−Hf−O angles in the hexamers of **6** and **7** are 177.1° 178.4°, respectively, while for HfO_2 the corresponding angle is 166.9°. The similarity in the local structure around Hf between these two cases provides a possible explanation to rationalize the formation of this planar hexamer.

The structures of the Hf clusters appear to be influenced, to some extent, by the ligation mode of the sulfates. Bridging μ_2-ligation is the predominant form of sulfate interaction as it promotes cluster growth. From this respect, sulfate can be compared to carboxylates that have been used to grow similar clusters.[4,12,17] μ_3-Sulfates also promote oligomerization, but they occur less frequently and appear to have a structure-directing effect on the cluster due to the rigid nature of a triply bridged Hf_3 unit. As discussed previously for the nonamer,[24] the formation of isolated octahedral hexamers in these solutions appears to be hindered by the μ_3-sulfates. Instead, larger clusters form containing a hexamer bridged to other motifs (e.g., 18-mer and 11-mer) or a nonamer cluster containing pentamers. The η_2-sulfates, unlike the other sulfates, appear to limit oligomerization. This can be clearly seen in the 11-mer, where four bidentate sulfates terminate the growth of the Hf ring that normally surrounds the hexamer in the 18-mer cluster.

Crystallization Regions. In this section, we relate the seven structures obtained to each other by inspecting the conditions under which they form. As previously noted, although the synthesis temperature played a role in the quality of crystals obtained, as defined by their size and ability to diffract X-rays, it did not influence the phase formed. For example, if crystals form from a solution at 60 °C, the same compound is obtained from this solution at 95 °C but in the form of smaller crystals. All crystals grown at elevated temperatures (60−95 °C) were of superior quality to those produced at room temperature; compounds **1**, **5**, **6**, and **7** crystallized *only* at elevated temperatures. For these reasons, we report only the results from the reactions at elevated temperatures. Compounds **1**−**4** crystallized at 60−95 °C, **5** required heating to 80−95 °C, and **6** and **7** crystallized only at 95 °C. Consequently, Figure 5 shows the crystallization regions of compounds **1**−**7** from sulfuric acid solutions with no further reference to synthesis temperature.

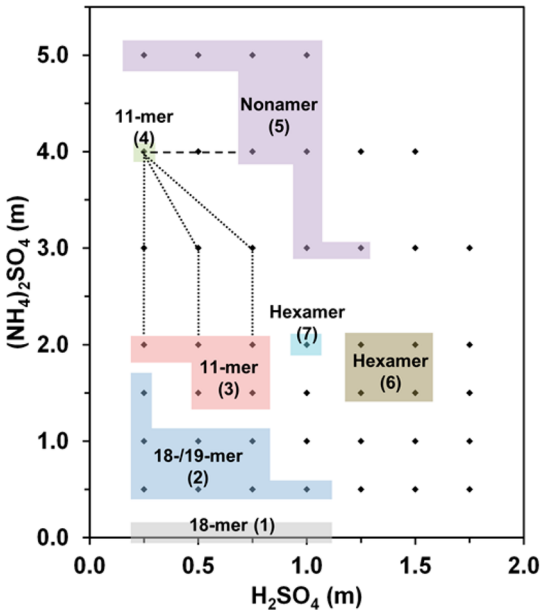

Figure 5. Crystallization regions of compounds **1**−**7** at 60−95 °C from sulfuric acid solutions. Each solution is represented by one point. Points linked by broken lines to two regions represent solutions from which both compounds crystallized.

The formation of hafnium oxo/hydroxo-clusters is confined to the acidic region 0.25 m < $[H_2SO_4]$ < 1.75 m. At lower acid concentrations rapid hydrolysis results in the precipitation of amorphous powders or the formation of gels. At higher acid concentration than covered by this range no crystallization is observed under our synthesis conditions. However, when the initially prepared acidic solutions were evaporated, crystals of various Hf sulfate salts form that contain no oxo/hydroxo connectivity (monomeric).[33−35] The clusters appear to occupy two regions. Compounds **1**−**5** crystallize from less acidic solutions, while **6** and **7** require slightly higher acidity. In the lower acidity region, a gradual decrease in cluster size is observed as the sulfate concentration is raised for fixed acid concentration. The largest clusters, 18-mers and 19-mers, appear at low sulfate. No $(NH_4)_2SO_4$ is required for the formation of **1**, but the addition of small amounts of the sulfate salt resulted in the formation of **2**, where the expanded unit cell causes the breaking of the sulfate bridge between the 18-mers. The incorporation of the additional $[SO_4]^{2-}$ and $[NH_4]^+$ into the voids between the clusters leads to this expansion.

Further addition of sulfate leads to more extensive complexation and the formation of smaller clusters. The 11-mer clusters form over a wide region of $[(NH_4)_2SO_4]$, with **3** dominating at the lower end, while further up **4** crystallizes. Compound **4** requires the incorporation of sulfate into the voids which explains why more sulfate is required in solution. Further increase in $[(NH_4)_2SO_4]$ results in the formation of the nonamer (**5**). The nonamer represents the upper limit of the

dx.doi.org/10.1021/ic501841e | Inorg. Chem. 2014, 53, 11252−11260

cluster size diminution. Reactions with higher sulfate concentration resulted in the crystallization of the nonamer. Reactions where a lower concentration of Hf was used, giving a higher $[(NH_4)_2SO_4]$/Hf ratio, also only resulted in the formation of **5**.

Upon increasing the acid concentration, the planar hexamer cluster can be accessed by crystallization of **6** and **7** in the regions shown in Figure 5. Compound **6** forms over a wider range of conditions compared to **7**, but in general both appear to be confined to limited range. It is intriguing that the hexamer, being the only cluster that does not share structural motifs with the other clusters, should form in a region isolated from the others. Not only is the structure of the planar hexamer considerably different from the others, the ratios of the coordinating ligands in this cluster are markedly dissimilar. Table 3 reveals trends in the larger (less acidic) clusters that are

Table 3. Ratios of Coordinated Ligands to Hf Atoms in the Clusters in Compounds 1−7

cluster	$[SO_4]^{2-}$/Hf	$[O]^{2-}$/Hf	$[OH]^{-}$/Hf	$[H_2O]$/Hf
18-mer (**1**)	0.71	0.56	1.44	1.11
18-mer (**2**)	0.72	0.56	1.44	1.22
19-mer (**2**)	0.68	0.58	1.42	1.16
11-mer (**3**, **4**)	1.36	0.64	1	0.55
nonamer (**5**)	1.56	0.89	0.67	0
planar hexamer (**6**, **7**)	1.75	0.83	0	1.08
$Hf(SO_4)_2{\cdot}4H_2O$[7]	2	0	0	4

not sustained by the planar hexamer. In the less acidic clusters, as the sulfate concentration (and hence complexation, second column) is increased, the extent of oxo-bridging increases, while those of hydroxo-bridging and H_2O coordination decrease. Increasing the sulfate complexation further requires the use of more acidic conditions, resulting in the planar hexamer formation. Although the $[OH]^-$/Hf ratio continues to drop, reaching zero for the hexamer, the other trends do not persist. There is a slight decrease in oxo-bridging, manifested in the formation of a planar rather than 3-dimentional core structure. Additionally, the hexamer contains a substantial amount of H_2O coordination, reversing the trend with cluster size. The hexamer appears to act as an intermediate state between the less acidic clusters and the more acidic monomeric species (lacking oxo/hydroxo bridging) that are obtained at high acid concentrations. The hafnium sulfate salt, $Hf(SO_4)_2{\cdot}4H_2O$,[7] is used as an example in Table 3 to demonstrate this.

The solutions at $[H_2SO_4]$ = 1 m show an interesting pattern of cluster formation as $[SO_4]^{2-}$ is increased. Instead of a gradual decrease in cluster size, the trend goes from 18-mers at $[(NH_4)_2SO_4]$ = 0−0.5 m, to the hexamer at 2 m, followed by the nonamer at >3 m. This abrupt switch between the clusters highlights the nonlinear nature of these crystallization regions, and may be related to the effect of varying $[(NH_4)_2SO_4]$ on the overall pH of these solutions. There appears to be some overlap between the region where the larger clusters form (**1**−**5**) and the more acidic region where the planar hexamers form. Both 18-mer and nonamer regions appear to extend slightly into more acidic conditions.

The advantage of using H_2SO_4 for the above study is that the acid does not add any other anions, which may incorporate in the crystal structures or affect the reagent solubility. Its limitation, however, is that increasing the acid concentration also raises the $[SO_4]^{2-}$ concentration in solution, rendering inaccessible the high acid/low sulfate region. For this reason, a similar study was conducted with HCl, as shown in Figure 6.

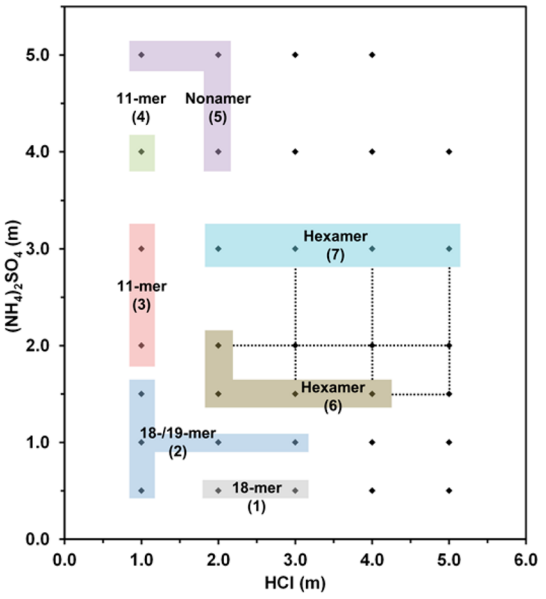

Figure 6. Crystallization regions of compounds **1**−**7** at 60−95 °C from hydrochloric acid solutions.

Cl^- is known to be less coordinating than $[SO_4]^{2-}$ and is already present in the solutions from the Hf precursor. In addition, it is known to be an effective cluster-capping ligand for the Pu 38-mer cluster.[16] Despite the high Cl^- concentration in the highly acidic solutions, we found no variation in the structures of compounds **1**−**7** between the two studies. The only changes appeared to be the size of the crystals grown. In particular, **1** and **3** formed much larger crystals in HCl than in H_2SO_4, facilitating their structure determination.

The HCl study reveals a similar pattern of the crystallization regions as that found for H_2SO_4. It confirmed that the clusters found in compounds **1**−**5** form in a less acidic region whereas the hexamer found in **6** and **7** crystallizes from more acidic solutions. The *x*-axis now represents the crystallization region of the tetramer, while compound **1** has moved up as it requires the presence of $[SO_4]^{2-}$ in solution. As before, the less acidic clusters (**1**−**5**) form in decreasing in size as $[SO_4]^{2-}$ is increased, with the nonamer representing the upper limit. The [HCl] = 2 m line represents the crossover into the more acidic regions where the planar hexamers appear. Incidentally, this represents the same $[H^+]$ concentration found in the $[H_2SO_4]$ = 1 m line in Figure 5 (presuming complete dissociation of the acids). A similar pattern of cluster formation is observed here, although the HCl case features both hexamer compounds **6** and **7**. Despite the similarities with the previous study, the use of HCl has a substantial effect on the planar hexamer crystallization regions **6** and **7**. These now span a much wider range in acidity and form even under very acidic conditions ([HCl] = 6 m). Compound **7**, containing the more ordered hexamer cluster arrangement, appears to form at higher $[SO_4]^{2-}$, although there is substantial overlap between **6** and **7** at lower $[SO_4]^{2-}$.

The formation of different compounds containing identical clusters indicates that they are present in solution but crystallize in different arrangements based on the solution conditions. In other words, the plots shown in Figures 5 and 6 not only reveal

dx.doi.org/10.1021/ic501841e | *Inorg. Chem.* 2014, 53, 11252−11260

the crystallization regions of **1**−**7**, but also indicate the stability regions of the four clusters in aqueous solutions. The occurrence of cocrystallization (as denoted by broken lines), particularly, between the 11-mer (**4**) and nonamer (**5**), suggests that different clusters can coexist in solution under specific conditions. Changing the acidity or sulfate concentration drives the hydrolysis and condensation equilibria in favor of one cluster over the other.

CONCLUSION

With the aid of the sulfate anion, hafnium forms a variety of oxo/hydroxo clusters in aqueous solutions with architectures that may appear random at first. However, upon close inspection, their structures can be related to one another as well as to dense HfO_2 phases. In this Article, the clusters that form below 100 °C were described. The study led to the discovery of another version of the 18-mer cluster, where the intercluster sulfate bridge is absent. This compound also contained small amounts of a new structurally related 19-mer species. Two compounds containing a novel 11-mer cluster were also reported. The 11-mer structure is a perfect fragment of the 18-mer, where the higher sulfate-to-hafnium appears to hinder the growth of the larger cluster. Finally, the structure of the previously described planar hexamer was re-examined, and a new crystal arrangement of this cluster was described.

The crystallization regions of these compounds were plotted against the concentrations of acid and sulfate. This led to informative plots wherein the structural features of the clusters can be related to the solution conditions under which they form. The more basic clusters, 18-mers, 19-mer, 11-mers, and nonamer form in a low acid region, whereby a clear decrease in cluster size is observed as $[SO_4]^{2-}$ is increased. It appears that the sulfate ligand, while promoting oligomerization of Hf in aqueous solutions, also impedes the growth of large clusters by complexing Hf more extensively and encasing the clusters. This strongly complexing ligand can be viewed as a catalyst for condensation reactions when present in small quantities, leading to large networks of oxo/hydroxo-bridged metal ions forming amorphous powders and gels. However, when present in significant quantities, the sulfate behaves as a reactive ligand that limits the growth of these networks in favor of discrete, well-defined clusters. Due to its ability to bridge three metal ions, the sulfate also appears to have a structure-directing effect on these clusters. The nonamer is the smallest species that can be obtained in low-acid conditions. Increasing the acidity, however, leads to the formation of the planar hexamer. It is clear from the distinctive structure of this latter cluster, and its stability under more acidic conditions, that it represents an intermediate state between the three-dimensional, cage-like, basic clusters and the simple hafnium sulfate salts containing no oxo/hydroxo-bridging.

Within the context of the role played by charge-density on competing olation versus oxolation condensation reactions, the results presented herein are obviously consistent with those observed in studying the 5f ions Th^{IV} and Pu^{IV}, both of which are softer than Hf^{IV}. The trend from smaller, hydroxo-bridged clusters to larger, oxo-bridged nanoparticles with increasing hardness does not manifest itself in this structural study. Instead, the reverse trend is observed; oxo-bridges are more prevalent in the smaller clusters. This result is not fundamentally understood, although it may reflect the lower coordination number associated with the d-block ions over their f-block counterparts. However, this is not consistent with the expected trend in metal acidity with ligation. Nevertheless, examining the crystal structures of clusters obtained from various aqueous solutions in a systematic fashion provides valuable information upon which to build an understanding of the species present in solution and their equilibria. Knowledge of these species and their properties is important for the development of aqueous synthesis and processing routes for metal oxides.

ASSOCIATED CONTENT

Supporting Information

Crystallographic data in CIF format. Synthetic procedures, crystallographic information, structure refinement details, and ORTEP illustrations for compounds **1**−**4**, **6**, and **7**. Solid-state Raman spectra. This material is available free of charge via the Internet at http://pubs.acs.org. Crystallographic data deposited with the Inorganic Crystal Structure Database (ICSD) at http://icsd.fiz-karlsruhe.de by referencing nos. 428123 (**1**), 428124 (**2**), 428125 (**3**), 428126 (**4**), 428127 (**6**), 428128 (**7**).

AUTHOR INFORMATION

Corresponding Author

*E-mail: LS@anl.gov.

Notes

The authors declare no competing financial interest.

ACKNOWLEDGMENTS

This work is supported by the U.S. Department of Energy, Office of Basic Energy Sciences under Contract DE-AC02-06CH11357.

REFERENCES

(1) Henry, M.; Jolivet, J. P.; Livage, J. In *Chemistry, Spectroscopy and Applications of Sol-Gel Glasses*; Reisfeld, R., Jørgensen, C. K., Eds.; Springer-Verlag: Berlin, 1992; p 153.
(2) Pope, M. T.; Muller, A. *Polyoxometalates: From Platonic Solids to Anti-Retroviral Activity*; Springer: New York, 1994.
(3) Clearfield, A. *Rev. Pure Appl. Chem.* **1964**, *14*, 91.
(4) Pan, L.; Heddy, R.; Li, J.; Zheng, C.; Huang, X.-Y.; Tang, X.; Kilpatrick, L. *Inorg. Chem.* **2008**, *47*, 5537.
(5) Pappas, I.; Fitzgerald, M.; Huang, X.-Y.; Li, J.; Pan, L. *Cryst. Growth Des.* **2009**, *9*, 5213−5219.
(6) Hu, Y.-J.; Knope, K. E.; Skanthakumar, S.; Kanatzidis, M. G.; Mitchell, J. F.; Soderholm, L. *J. Am. Chem. Soc.* **2013**, *135*, 14240.
(7) Kalaji, A.; Skanthakumar, S.; Kanatzidis, M. G.; Mitchell, J. F.; Soderholm, L. *Inorg. Chem.* **2014**, *53*, 6321.
(8) Johnson, G. L.; Toth, L. M. *Plutonium(IV) and Thorium(IV) Hydrous Polymer Chemistry*; ORNL/TM-6365; 1978.
(9) Knope, K. E.; Soderholm, L. *Chem. Rev.* **2013**, *113*, 944−994.
(10) Wilson, R. E.; Skanthakumar, S.; Sigmon, G.; Burns, P. C.; Soderholm, L. *Inorg. Chem.* **2007**, *46*, 2368−2372.
(11) Soderholm, L.; Almond, P. M.; Skanthakumar, S.; Wilson, R. E.; Burns, P. C. *Angew. Chem., Int. Ed.* **2008**, *47*, 298−302.
(12) Knope, K. E.; Wilson, R. E.; Vasiliu, M.; Dixon, D. A.; Soderholm, L. *Inorg. Chem.* **2011**, *50*, 9696.
(13) Knope, K. E.; Vasiliu, M.; Dixon, D. A.; Soderholm, L. *Inorg. Chem.* **2012**, *51*, 4239−4249.
(14) Hennig, C.; Takao, S.; Takao, K.; Weiss, S.; Kraus, W.; Emmerling, F.; Scheinost, A. C. *Dalton Trans.* **2012**, *41*, 12818−12823.
(15) Knope, K. E.; Soderholm, L. *Inorg. Chem.* **2013**, *52*, 6770−6772.
(16) Wilson, R. E.; Skanthakumar, S.; Soderholm, L. *Angew. Chem., Int. Ed.* **2011**, *50*, 11234−11237.
(17) Hu, Y.-J.; Knope, K. E.; Skanthakumar, S.; Soderholm, L. *Eur. J. Inorg. Chem.* **2013**, *2013*, 4159.
(18) Hagfeldt, C.; Kessler, V.; Persson, I. *Dalton Trans.* **2004**, 2142.

(19) Godneva, M. M.; Motov, D. L.; Kuznetsov, V. Y. *Russ. J. Inorg. Chem.* **2003**, *48*, 112.
(20) Squattrito, P. J.; Rudolf, P. R.; Clearfield, A. *Inorg. Chem.* **1987**, *26*, 4240.
(21) Kuznetsov, V. Y.; Dikareva, L. M.; Rogachev, D. L.; Porai-Koshits, M. A. *J. Struct. Chem.* **1985**, *26*, 923.
(22) Mark, W.; Hansson, M. *Acta Crystallogr., Sect. B* **1975**, *31*, 1101.
(23) Dalgarno, S. J.; Atwood, J. L.; Raston, C. L. *Inorg. Chim. Acta* **2007**, *360*, 1344.
(24) Kalaji, A.; Soderholm, L. *Chem. Commun.* **2014**, *50*, 997.
(25) Choi, J. H.; Mao, Y.; Chang, J. P. *Mater. Sci. Eng., R* **2011**, *72*, 97.
(26) Li, F. M.; Bayer, B. C.; Hofmann, S.; Dutson, J. D.; Wakeham, S. J.; Thwaites, M. J.; Milne, W. I.; Flewitt, A. J. *Appl. Phys. Lett.* **2011**, *98*, 252903.
(27) Brese, N. E.; O'Keeffe, M. *Acta Crystallogr., Sect. B* **1991**, *47*, 192.
(28) Vasiliu, M.; Knope, K. E.; Soderholm, L.; Dixon, D. A. *J. Phys. Chem. A* **2012**, *116*, 6917−6926.
(29) Takao, K.; Takao, S.; Scheinost, A. C.; Bernhard, G.; Hennig, C. *Inorg. Chem.* **2012**, *51*, 1336−1344.
(30) Falaise, C.; Volkringer, C.; Loiseau, T. *Cryst. Growth Des.* **2013**, *13*, 3225−3231.
(31) Ruh, R.; Corfield, P. W. R. *J. Am. Chem. Soc.* **1970**, *53*, 126.
(32) Kuznetsov, V. Y.; Dikareva, L. M.; Rogachev, D. L.; Nikolaev, V. P.; Porai-Koshits, M. A. *J. Struct. Chem.* **1984**, *25*, 968.
(33) Sozinova, Y. P.; Motov, D. L. *Russ. J. Inorg. Chem.* **1978**, *23*, 609.
(34) Rogachev, D. L.; Dikareva, L. M.; Kuznetsov, V. Y.; Fomenko, V. V.; Porai-Koshits, M. A. *J. Struct. Chem.* **1982**, *23*, 765.
(35) Kuznetsov, V. Y.; Rogachev, D. L.; Dikareva, L. M.; Porai-Koshits, M. A. *J. Struct. Chem.* **1985**, *26*, 225.